



## Microstate analysis in infancy

Kara L. Brown <sup>\*</sup>, Maria A. Gartstein

Department of Psychology, Washington State University, USA



### ARTICLE INFO

**Keywords:**

Infancy  
Microstates  
EEG  
Development  
Resting-state

### ABSTRACT

**Background:** Microstate analysis is an emerging method for investigating global brain connections using electroencephalography (EEG). Microstates have been colloquially referred to as the “atom of thought,” meaning that from these underlying networks comes coordinated neural processing and cognition. The present study examined microstates at 6-, 8-, and 10-months of age. It was hypothesized that infants would demonstrate distinct microstates comparable to those identified in adults that also parallel resting-state networks using fMRI. An additional exploratory aim was to examine the relationship between microstates and temperament, assessed via parent reports, to further demonstrate microstate analysis as a viable tool for examining the relationship between neural networks, cognitive processes as well as emotional expression embodied in temperament attributes.

**Methods:** The microstates analysis was performed with infant EEG data when the infant was either 6- ( $n = 12$ ), 8- ( $n = 16$ ), or 10-months ( $n = 6$ ) old. The resting-state task involved watching a 1-minute video segment of Baby Einstein while listening to the accompanying music. Parents completed the IBQ-R to assess infant temperament.

**Results:** Four microstate topographies were extracted. Microstate 1 had an isolated posterior activation; Microstate 2 had a symmetric occipital to prefrontal orientation; Microstate 3 had a left occipital to right frontal orientation; and Microstate 4 had a right occipital to left frontal orientation. At 10-months old, Microstate 3, thought to reflect auditory/language processing, became activated more often, for longer periods of time, covering significantly more time across the task and was more likely to be transitioned into. This finding is interpreted as consistent with language acquisition and phonological processing that emerges around 10-months. Microstate topographies and parameters were also correlated with differing temperament broadband and narrowband scales on the IBQ-R.

**Conclusion:** Three microstates emerged that appear comparable to underlying networks identified in adult and infant microstate literature and fMRI studies. Each of the temperament domains was related to specific microstates and their parameters. These networks also correspond with auditory and visual processing as well as the default mode network found in prior research and can lead to new investigations examining differences across stimulus presentations to further explain how infants begin to recognize, respond to, and engage with the world around them.

<sup>\*</sup> Correspondence to: Washington State University, PO Box 644820, Pullman, WA 99164-4820, USA.  
E-mail address: [Kara.Brown@wsu.edu](mailto:Kara.Brown@wsu.edu) (K.L. Brown).

## 1. Introduction

There has been growing interest in examining whole-brain processes during the resting state because of paradigm shifts emphasizing underlying neural networks (Mesulam, 2012; Meehan, Bressler, 2012) and the complexity of their activity even during periods of limited external stimulation (Fox & Raichle, 2007; Greicius et al., 2002). In their seminal paper Lehmann and colleagues (1987) discuss functional networks in the brain and the importance of examining these globally, using EEG. Following this approach, they found a limited number of discrete, stable states, hypothesizing that these stem from functional states and lead to different effects on information processing (Lehmann et al., 1987). These states are termed microstates and have been described as the “atom of thought,” meaning that from a specific coordination of neural activity stems basic information processing, including processing of emotionally salient stimuli and cognition (Lehmann et al., 1998). It has been hypothesized that microstate emergence corresponds to integration of the environmental stimuli with emotions and cognitions, such as one’s internal state and previous knowledge, giving rise to consciousness (Milz et al., 2016; Michel & Koenig, 2018). This integration is done on a millisecond-by-millisecond basis, with many microstates occurring and reoccurring within just one second given that microstates last between 80 and 120 ms, much faster than what is detected with BOLD signal from fMRI (Koenig et al., 2002; Britz et al., 2010). The growing interest in examining resting states has contributed to a wider application of the microstates methodology, identifying distinct patterns of EEG activity distributed spatially over the scalp thought to be related to underlying neural activity and functional processes found with fMRI.

Since Lehmann’s groundbreaking discovery, there has been a growing body of research examining microstates, mostly focused in healthy adult populations. (Gianotti et al., 2008) examined microstates in the context of emotionally salient stimuli in adults. They found patterns of activation of certain microstates related to valence of emotion (positive vs negative) and the arousal level (high vs low). Specifically, underlying networks for processing valence and arousal were associated with different microstates, with valence prioritized for processing followed by arousal. Zerna and colleagues (2021) reported that microstates were implicated in processing positive and negative emotions above and beyond what has been found in event-related potential work, meaning that there are both local and global network differences for processing different emotions. Kaur and colleagues (2020) reported that, in an adult population, microstates-based asymmetry correlated with neural mechanisms of negative affect (e.g., alpha-BOLD synchronization). However, there were no reliable correlations with positive affect, the behavioral inhibition system (BIS), and the behavioral activation system (BAS) functioning, indicating that microstate analysis might be useful for identifying only some neural underpinning of emotionality (Kaur et al., 2020). Of note, EEG alpha asymmetry has been a widely used tool in infant populations for measuring approach/avoidance (see Smith et al., 2017 for review). This recent work shows that microstate analysis has the potential to uncover patterns of global brain activity related to underlying cognition and neural processing of specific emotions, enhancing our understanding of their temporal unfolding. In addition to healthy adult populations, microstate analysis has recently been utilized to elucidate endophenotypes for a variety of disorders including schizophrenia (e.g., Da Cruz et al., 2020), depression (Murphy et al., 2020), and autism spectrum disorder (ASD; Jia & Yu, 2018), each with significant impacts on emotionality.

While research on microstates in children is limited, a notable cross-sectional investigation examined microstates across the lifespan. Koenig and colleagues (2002) considered microstates across ages ranging from 6 to 80 years old. Four discrete microstates were observed across this age range and corresponded with topographies closely matching microstates from previous work (Michel & Koenig, 2018). At the same time, microstate profiles varied across age groups; some microstates dominated during certain age ranges, with a declining presence in other age groups. Longer durations of microstates were also observed in younger children as compared to adult microstates (Koenig et al., 2002). Researchers proposed that these shifts correspond with developmental transitions in neural processing linked to changes in emotions, cognition, and behavior.

In infancy, Khazaei et al. (2021) utilized microstate analysis during REM and NREM sleep to discern the functional organization and dynamic changes in the brain. Seven microstates dominated in this sample of 60 full-term infants, rather than four typically reported in the adult microstate literature (Michel & Koenig, 2018). Additionally, they found that the sequences of microstate transitions and certain microstate parameters (duration and occurrence) differed depending on whether the infant was in an active state or quiet state of sleep. Maitre et al. (2020) examined microstates in full-term and preterm neonates and found differences in the brain’s response to multisensory stimuli across these groups, implicated in later sensory and internalizing tendencies. Further, they found that three different microstate topographies characterized brain responses during the task. In a recent study, Gui et al. (2021) observed four microstates in infancy that corresponded with social attention and later potential emergence of ASD. These studies support the feasibility of identifying microstates in infancy and point to the potential use of microstate analysis to predict functional brain dynamics and later developmental trajectories. Importantly, microstates appear to be promising biomarkers for the development of typical and atypical neural functioning across many domains including executive functioning and emotional development, pointing to the importance of better understanding microstates during a wakeful resting task in infants.

It was originally thought that the brain at rest was unorganized and random, only to take on a structured organization when presented with a stimulus. Through fMRI studies, however, it was discerned that the resting state involved synchronization in a network later termed the default mode network (Biswal et al., 1995; Raichle et al., 2001). More recent research points to the resting state as inhibition rather than a “default state,” again indicating that the coordination of underlying activity is purposeful (Camacho et al., 2020; Whedon et al., 2020). It quickly became evident that the resting state was more than the brain at rest.

Fransson et al. (2007) examined resting state networks in terms of their functional connections for pre-term infants using fMRI. They found five resting-state networks in the infant brain that overlapped with observations in the adult literature, noting evidence for the emergence of long-range functional connectivity early in development and strengthening with age (2007). Honing in on resting networks further, Gao et al. (2015), again using fMRI, found variability in developmental timing of resting state networks wherein these emerged at different times during the first year of life. This pattern of variable trajectories in turn suggests that different

neurodevelopmental processes are likely associated with these shifts, possibly coinciding with brain maturation, as well as changes in emotions, cognition, and behavior.

While fMRI studies have been utilized most often to examine these global neural connections, some limitations associated with this approach should be noted. As fMRI studies require stillness to obtain usable data, it is typical for infants to be asleep to maintain the required motionless state. The sleep state significantly limits research questions that can be explored, including those regarding brain activity during a wakeful resting state (i.e., quiet alert state). Perhaps most importantly, having the infants sleeping raises concern about comparisons to older children and adults who are awake during resting state recordings. Additionally, while there have been advancements in temporal resolution with fMRI, the Blood-Oxygen-Level-Dependent (BOLD) response is too slow to gain temporal acuity in regard to cognitive and emotional processes (Mele et al., 2019). Although fMRI does have advantages such as spatial resolution, sole use of fMRI to examine infant neural connectivity leaves many questions unanswered.

Electroencephalography (EEG) represents a non-invasive alternative to address questions regarding neural functioning in humans and to minimize the limitations of fMRI. This method provides an ability to record neural activity by quantifying the electric flow throughout the brain in both a local (over cortical regions of interest) and global (whole brain patterns of activity) manner. EEG does not require the level of inactivity for data acquisition needed in fMRI studies. In fact, it is possible to have similar conditions for a resting state condition across the lifespan when using EEG. Additionally, recording signals while the infant is awake presents an opportunity to ask a wider array of research questions and provides a more optimal parallel to studies of adult resting state networks. EEG also allows for superior temporal specificity and can provide greater temporal resolution for examining the rapidly changing network shifts.

While microstates have been examined across a wide age range and in infancy during specific tasks (e.g., social, sensory, sleep), microstate analysis has not yet been conducted in the second half of the first year of life in a wakeful resting-state task. This developmental period is of particular interest as infants are beginning to engage with the world around them to a greater extent. By comparing microstates in infants across this timeframe, the emergence of early neurodevelopmental processes can be elucidated, with potential biomarkers identified for use in research addressing lifespan neural network development. Delineating how microstates emerge is also important as these are understood as providing the foundation for consciousness (Lehmann et al., 1998) and related cognitive and affective processes. The mid-to-late infancy period is active with respect to emotional development, with evolving social understanding and transitions in reactivity and regulation (Rosenblum et al., 2019). Microstates elucidated during a “baseline task” designed to induce a calm/alert state may be more consistently linked with information processing and behavioral tendencies reflected in temperament attributes.

According to Rothbart's psychobiological framework, temperament is defined as constitutionally based individual differences that incorporate reactivity along with attention-based regulation, both informed by one's biological makeup and impacted by maturation and environment (Rothbart & Derryberry, 1981). Along with motivational-affective systems responsible for approach/avoidance (and associated positive and negative emotionality), this definition of temperament incorporates a regulation-related domain supported by attentional skills, long considered as cognitive functions (Rothbart et al., 2006). Because microstates are thought of as indicators of ongoing global brain activity reflecting cognitive and emotional elements, their links with temperament, also encompassing emotional and cognitive attributes, represents an important next step in research. That is, temperament traits can be expected to predispose individuals to experience certain microstates differently, leading to differential associations with their parameters.

Microstate analyses provide researchers with an abundance of information beginning with the microstates that best represent the data. The topographical shapes of the microstates often provide the basis for comparisons across groups and are used to theorize about the functionality of the microstates. Many studies have identified the same four microstates (termed A, B, C, and D) that show distinct topography (see Michel & Koenig, 2018 for review). The duration of microstates throughout the recording period and frequency of switching between microstates are also typically considered. Specifically, duration of microstates has been defined as the stability of the microstate when it appears based on the average time spent in that microstate, and the frequency of a microstate appearance is thought to represent the tendency for the underlying neurological networks to become activated (Khanna et al., 2014). Duration and frequency of microstates were shown to characterize different neuropsychiatric diseases including schizophrenia (Lehmann et al. 2005), depression (Strik et al., 1995) and panic disorder (Kikuchi et al., 2011). Thus, duration and frequency each address certain aspects of stability and transformation of brain activity states and are important for understanding the underlying neurological processes. Additionally, coverage is often examined to understand how much time each microstate takes up of the total amount of recording time (Lehmann et al. 1987). Coverage is thought to represent the relative presence with respect to other microstates and perhaps a more stable pattern of network activation (Croce et al., 2020). Amplitude is also considered, which is the average global field power during microstate dominance (Strelts et al., 2003). This gives insight into the strength of activation of the underlying networks. Global explained variance (GEV) is the percentage of the total variance explained by each microstate, or how much of the data is represented by this microstate (Brodtbeck et al., 2012). Lastly, transition probabilities can be informative by examining the likelihood of switching from one microstate to another (Lehmann et al., 2005). Each of these parameters provide a better understanding of the underlying microstates and resting state networks.

This study was designed to discern infant microstates in the second half of the first year of life, when origins of later developing executive functions and self-regulatory processes are thought to “come online”, providing the basis for more advanced social-emotional development (Cuevas & Bell, 2014). Specifically, this project will shed light on differentiation of brain networks, as well as their connectivity, with implications for cognitive and emotional/motivational processes. Based on prior research examining microstates from infancy to adulthood (Koenig et al., 2002; Khanna et al., 2015; Gui et al., 2021; Maitre et al., 2021) as well as comparative research addressing similarities of resting state networks in adults and infants using fMRI, it is hypothesized that infants will show distinct microstates. Specifically, EEG data from infants will show distinct microstates that can subsequently be compared to

the microstates documented in adult populations and later examined in the context of stimulus presentations. We used a cross-sectional design to better understand at what timepoints microstates can be reliably identified and if there are differences in microstates parameters across the second half of the first year.

As an exploratory aspect of this study, infant temperament measured via the Infant Behavior Questionnaire Revised (IBQ-R; [Gartstein & Rothbart, 2003](#)) will be examined in a subset of infants ( $n = 25$ ) whose parents completed the questionnaire to explore potential relationships between temperament and microstates. The IBQ-R is a parent-report measure of infant temperament with a hierarchical structure wherein each of the three broadband factors is comprised of multiple narrowband scales: Surgency/Positive Affectivity (Approach, Vocal Reactivity, Smiling and Laughter, High-Intensity Pleasure, Perceptual Sensitivity, Activity); Negative Emotionality (Distress to Limitations, Fear, Sadness, Falling Reactivity); and Regulatory Capacity/Orienting (Duration of Orienting, Cuddliness, Soothability, and Low-Intensity Pleasure). Temperament profiles provide an important window into emotional development, motivation, self-regulation, attention, and related cognitive processes. If aspects of temperament can be shown as associated with specific microstates and their parameters herein, we can begin to elucidate biological foundations of temperament and related emotional and cognitive processes using a whole-brain system to identify key contributors to development. While we expected a number of such associations to emerge, specific hypotheses could not be formulated because of the lack of sufficient prior research.

## 2. Methods

### 2.1. Participants

Mother-infant dyads were recruited from the Eastern Washington/Northern Idaho area and participated when the infant was either 6 months ( $n = 18$ ), 8 months ( $n = 17$ ), or 10 months ( $n = 15$ ) of age with a range of two weeks around each time point to allow for some flexibility with scheduling while also maintaining the integrity of each age group. The present study incorporated a subset of a previously described dataset ( $n = 59$ ; [Gartstein, 2019](#); [Campagna et al., 2021](#)), as well as a portion of the ongoing longitudinal data collection effort ( $n = 39$ ), reporting cross-sectional data only due to the preliminary/in-progress status of follow-up evaluations. Only families with healthy (e.g., absence of medical or birth complications) infants were eligible to participate in this study. Mothers with infants who met criteria were invited to the research lab to complete the study. For the purposes of this study, we were only interested in baseline, or resting state data, which were collected immediately after the placement of the EEG cap and involved the infant watching a 1-minute clip of Baby Einstein. Although adults can be told to simply sit still (with their eyes open or closed) to achieve a quiet alert state, infants must be provided with a calm activity, typically involving visually presented stimuli ([Anderson & Perone, 2018](#)). Infants who participated but did not have a sufficient amount of baseline EEG data (baseline EEG data lasting less than 45 s) were excluded from microstate analyses ( $n = 9$ ). The baseline procedure was time-locked to the EEG recording using E-Prime (Psychology Software Tools, Inc.) by transmitting triggers initiated by specific keyboard presses. These triggers were sent to the BioSemi acquisition software, marking the beginning and ending times for the baseline task within the EEG data.

### 2.2. EEG recording

Before the baseline task was started, an infant 32-electrode EEG cap (Cortech Solutions, Inc.; Wilmington, NC) was placed on the infant's head. After cap placement, electro-conductive gel was injected at each of the electrode sites. The individual electrodes (BioSemi – Cortech Solutions, Inc.; Wilmington, NC) were then placed into their corresponding section on the cap for EEG recording of frontal, mediofrontal, lateral frontal, central, temporal, parietal, and occipital areas. The EEG data were collected using the BioSemi Active Two amplifier. To examine scalp connection, an initial screening of impedances was conducted. The Biosemi acquisition software was set at a sampling rate of 256 Hz and the electrodes were referenced to Cz during recording.

### 2.3. EEG data processing

Data were digitally filtered from 1 Hz to 50 Hz using the ERPLAB plugin ([Lopez-Calderon & Luck, 2014](#)) to account for the slower frequencies seen in infant populations, as well as account for 60hz environmental electrical activity. While 1hz filtering is typical in infant populations ([Cherian et al., 2009](#); [Britton et al., 2016](#)), a 1hz filter was used for this study because of the use of ICA. When utilizing ICA, a filter of 1hz or greater decreases the signal-to-noise ratio and increases classification accuracy ([Winkler et al., 2015](#)). Using the TrimOutlier plugin in EEGLab (TrimOutlier plugin: <https://sccn.ucsd.edu/wiki/TrimOutlier>), data was inspected for channels that exceeded a differential average amplitude of 150  $\mu$ V. These malfunctioning electrodes were removed (on average, 0.74 electrodes were removed per participant and later interpolated), as to not impact the independent component analysis (ICA) by introducing non-linearities into the data. Any data that required interpolation of more than 10% of channels (3 EEG channels) was deemed unusable, and that data was removed from analyses. A total of 6 subjects (two 6-month, one 8-month, and three 10-month) were removed at this point in processing. Movement, cap placement, sensor, and other artifact were removed using ICA (Infomax) implemented in EEGLAB ([Delorme & Makeig, 2004](#)) using Matlab (The MathWorks, Natick, MA, United States). ICA component removal was used as sparingly as possible to keep as much data as possible for each participant (on average, 9 components were removed per participant). Participants with data that were too artifact-laden and required the removal of over 33% of components were removed at this point in data processing. A total of 10 subjects' data (four 6-month and six 10-month) were removed at this point in processing. Given the need for continuous EEG data for the microstates analysis in this project, ICA was utilized to clean the data (i.e., rather than removing problematic epochs entirely). After this point in data processing, the final sample included 34 infants

(6-months,  $n = 12$ ; 8-month,  $n = 16$ ; 10-month,  $n = 6$ ). Because continuous data was used, transition probabilities were able to be extracted and analyzed. Additionally, this allowed to keep the entire 60-second time window for microstate analysis for each subject with useable EEG data.

After ICA component removal, the eliminated electrodes were added back for further analyses - interpolated based on the cleaned data. Data were then average referenced, meaning that all electrical activity from each of the 32 electrodes were averaged together, and that average was then subtracted from each electrode. This method decreases the amplitude across the scalp but allows each electrode to contribute equally to the reference. Because we are interested in the global picture of electrical activity, an average reference will allow for each electrode to contribute equally to gain a better understanding of the displacement of electrical activity across the entirety of the scalp area.

#### 2.4. Microstate analysis

From this previously collected and processed EEG data, the Global Field Power (GFP) - the standard deviation of the potential field during baseline/resting state, was computed. This allows for the examination of the natural resting microstate fluctuations. Using a more recent development in microstate analysis known as clustering analysis, topographies at all GFP peaks were simultaneously extracted and grouped into small classes based on their topographic similarities (Pascual-Marqui et al., 1995). Specifically, Atomize and Agglomerate Hierarchical Clustering, a class of clustering analysis, was used to cluster the microstate topographies. It then identifies the “worst” cluster, or the least representative cluster, and atomizes it, reassigning the members to the clusters that are most similar (Poulsen et al., 2018). From this classification, the microstate topographies were placed back into sequential order to determine the natural progression and amount of time spent in each of the microstates. These patterns were statistically compared across each time period (6-, 8-, and 10-months), and descriptively to those previously reported for adult microstates (Khanna et al., 2015).

#### 2.5. Statistical analyses

IBM SPSS statistics v. 27 was used to compute descriptive statistics and analysis of variance (ANOVA). ANOVA was utilized to compare across microstate topographies and across age groups. Specifically, a two-way mixed model (one-between/one-within) ANOVA was used to compare microstate parameters (amplitude, duration, and frequency) as well as GEV across the three age groups (6, 8, and 10-months), with microstate indicators as repeated measures, as is the usual approach in the literature (Lehmann, 2005). Because coverage is broken down into percentages of time of the whole baseline task and the microstates’ coverage when summed together equals 100, there is no variance when collapsing across microstate topographies and comparing this parameter between ages. Therefore, a two-way mixed model ANOVA was not able to be utilized for this parameter. Instead, coverage was compared using a one-way between-group ANOVA for each microstate topography across ages, then percentages are reported for each microstate topography at each age group. Utilizing a one-way ANOVA, the typical sequence of microstates was also examined across the three age groups, with transition probabilities examined for each microstate topography.

For the exploratory analyses, SPSS v. 27 was used to compute bivariate correlations between microstate parameters (GFP, duration, frequency, coverage) for each of the four microstates and broadband domains from the IBQ-R. Narrowband domains from the IBQ-R were examined only if there were significant correlations at the broadband level.

### 3. Results

Fig. 1 shows the topographies of the four microstates identified in infancy. With the exception of Microstate 1, they closely replicate topographies found in previous work (Koenig et al., 2002). Microstate 1 did closely replicate a microstate found by Gui et al. (2021) in a population of 8-month infants, but they did not consider this topography to be representative, as it was only found in a subset of their sample. Microstate 1 has a posterior activation, Microstate 2 has a symmetric occipital to prefrontal orientation, Microstate 3 has a left occipital to right frontal orientation, and Microstate 4 has a right occipital to left frontal orientation.

#### 3.1. Amplitude/GFP

Average amplitude/GFP for the microstates is reported in Table 1. A two-way mixed methods ANOVA was performed to compare the effects of age and microstate topography on amplitude, a measure of average global field power (Table 2). Because the results of Mauchly’s test were significant ( $\chi^2(5) = 44.24$ ,  $p > .001$ ), indicating that the assumption of sphericity was violated, the Grenhouse-

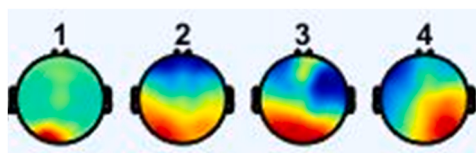


**Fig. 1.** Microstate Topographies with ICA. Note. Topographical maps of the four microstate classes (1–4). Map areas of opposite polarity are arbitrarily coded in red and blue, left ear is left, nose is up.

**Table 1**

Descriptive statistics for parameters at each age and for each microstate.

Age	6-months	8-months	10-months	Total
GFP1	14.79 (3.98)	15.18 (6.02)	16.13 (2.36)	15.21 (4.77)
GFP2	13.96 (2.82)	14.88 (2.49)	15.98 (2.09)	14.75 (2.58)
GFP3	13.96 (2.50)	15.05 (4.34)	16.31 (2.67)	14.89 (3.53)
GFP4	13.04 (2.17)	13.57 (2.27)	14.76 (2.42)	13.59 (2.27)
Duration 1	83.35 (14.04)	82.82 (11.54)	72.39 (10.72)	81.17 (12.68)
Duration 2	99.38 (11.11)	96.00 (13.29)	90.14 (26.35)	96.16 (15.39)
Duration 3	83.60 (9.78)	84.59 (16.77)	118.95 (63.70)	90.19 (30.94)
Duration 4	93.34 (8.48)	86.83 (5.36)	80.71 (8.17)	88.05 (8.24)
Frequency 1	2.03 (0.43)	2.43 (0.48)	1.52 (0.42)	2.13 (0.56)
Frequency 2	3.18 (0.39)	3.08 (0.79)	2.71 (1.46)	3.05 (0.83)
Frequency 3	2.57 (0.43)	2.48 (0.65)	2.89 (0.36)	2.58 (0.54)
Frequency 4	3.19 (0.32)	3.14 (0.35)	3.08 (0.46)	3.15 (0.35)
GEV 1	0.060 (0.06)	0.072 (0.10)	0.043 (0.05)	0.063 (0.08)
GEV 2	0.095 (0.03)	0.104 (0.06)	0.098 (0.07)	0.100 (0.05)
GEV 3	0.057 (0.03)	0.054 (0.03)	0.144 (0.14)	0.071 (0.07)
GEV 4	0.056 (0.01)	0.065 (0.04)	0.054 (0.03)	0.060 (0.03)

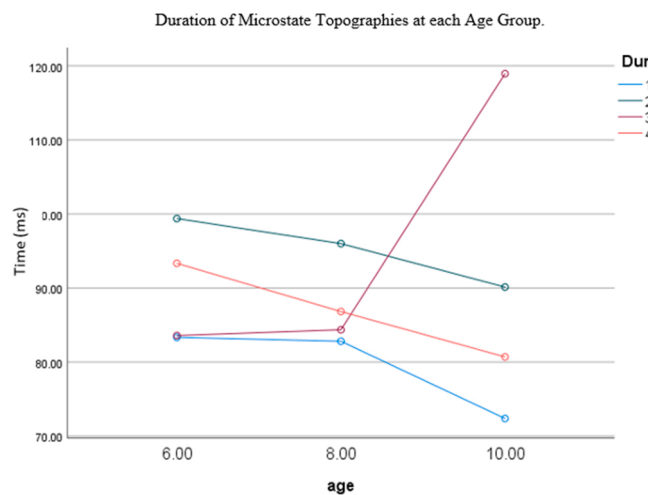
Note. The numbers in the first column correspond with one of the four microstate topographies. Mean (SD).

**Table 2**

ANOVA for Microstate Parameters with regard to Age and Microstate Topography.

	df	F	P value
GFP/Amplitude			
Age	2	0.86	0.43
Topography	1.86	2.60	0.09
Age*Topography	3.71	0.10	0.98
Duration			
Age	2	0.91	0.41
Topography	1.38	4.45	0.03 *
Age*Topography	2.77	3.24	0.03 *
Frequency			
Age	2	2.42	0.10
Topography	1.63	19.81	> 0.001 *
Age*Topography	3.27	1.99	0.12
GEV			
Age	2	1.68	0.20
Topography	2.22	2.91	0.06
Age*Topography	4.45	1.62	0.74

Note. Results of the ANOVAs of microstate GFP, Duration, Frequency, and GEV using age as independent variable and microstate topography as repeated measure.

**Fig. 2.** Duration of Microstate Topographies at each Age Group.

Giesser correction statistics are reported. A two-way mixed methods ANOVA revealed there was not a significant difference for amplitude across ages ( $F(2) = 0.86, p = .43, \eta_p^2 = .05$ ) or microstate topographies ( $F(1.86) = 2.60, p = .09, \eta_p^2 = .08$ ). There was also not a significant interaction between age and topography ( $F(3.15) = 0.098, p = .99, \eta_p^2 = .006$ ). This indicates that amplitude remains fairly stable over microstate topographies within each age group and does not differ across 6-, 8-, and 10-months.

### 3.2. Duration

Average duration of microstates is reported in [Table 1](#). Differences in duration, a measure of the average time spent in a particular microstate, emerged for microstate topographies across ages ([Table 2](#)). A two-way mixed methods ANOVA was performed to compare the effects of age and microstate topography on Duration. Because the results of Mauchly's test were significant ( $\chi^2(5) = 63.32, p > .001$ ), indicating that the assumption of sphericity was violated, the Grenhouse-Giesser correction is reported. A two-way mixed methods ANOVA revealed there was a significant interaction between age and topography for duration ( $F(2.77) = 3.24, p = .03, \eta_p^2 = .17$ ), indicating that Duration of certain microstates differed as a function of age. Specifically, Microstate 3 was found to have an increased duration at 10-months compared to 6- and 8-months while all other microstate topographies remained fairly stable in duration across age groups ([Fig. 2](#)).

### 3.3. Frequency

Average frequencies for the microstates are reported in [Table 1](#). Analysis of Frequency, a measure of how often the microstate would become activated, showed an interesting interaction between microstate topographies as a function of age ([Table 2](#)). A two-way mixed methods ANOVA was performed to compare the effects of age and microstate topography on Frequency. Because the results of Mauchly's test were significant ( $\chi^2(5) = 54.94, p > .001$ ), indicating that the assumption of sphericity was violated, the Grenhouse-Giesser correction is again reported. A two-way mixed methods ANOVA revealed there was no significant effect of age ( $F(2) = 2.42, p = .11, \eta_p^2 = .14$ ) nor was there a significant interaction between Frequency and age ( $F(3.27) = 1.99, p = .12, \eta_p^2 = .11$ ). There was a significant main effect for topography ( $F(1.63) = 19.81, p > .001, \eta_p^2 = .39$ ), indicating that the frequency of certain microstates differed from other microstate frequencies. Specifically, differences in frequency occurred between microstates 1 and 2 ( $p > .001$ , 95% C.I. =  $[-1.39, -0.60]$ ), between microstates 1 and 3 ( $p > .001$ , 95% C.I. =  $[-0.91, -0.39]$ ), between microstates 1 and 4 ( $p > .001$ , 95% C.I. =  $[-1.41, -0.89]$ ), and between microstates 3 and 4 ( $p = .001$ , 95% C.I. =  $[-0.75, -0.23]$ ). The frequency of microstate 1 was significantly lower than the frequencies of microstates 2, 3, and 4, and microstate 3 was significantly lower than microstate 4 ([Fig. 3](#)).

### 3.4. Global explained variance (GEV)

GEV, a measure of the total variance explained by each microstate, did not differ across ages or topographies ([Table 2](#)). A two-way mixed methods ANOVA was performed to compare the effects of age and microstate topography on GEV. Because the results of Mauchly's test were significant ( $\chi^2(5) = 30.85, p > .001$ ), indicating that the assumption of sphericity was violated, the Grenhouse-Giesser correction is reported. A two-way mixed methods ANOVA revealed there was not a significant difference for GEV across ages ( $F(2) = 1.68, p = .20, \eta_p^2 = .10$ ) or microstate topographies ( $F(2.22) = 2.91, p = .06, \eta_p^2 = .09$ ). There was also not a significant interaction between age and topography ( $F(4.45) = 1.62, p = .17, \eta_p^2 = .10$ ). This indicates that GEV remains fairly stable over

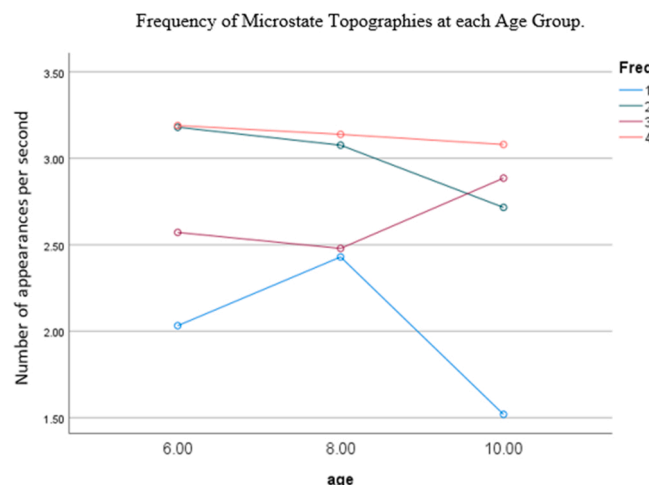


**Fig. 3.** Frequency of Microstate Topographies at each Age Group.

microstate topographies within each age group and does not differ across 6-, 8-, and 10-months.

### 3.5. Coverage

Because coverage is reported as percentages of the time window, a one-way ANOVA was performed to compare the effect of age on coverage for each microstate topography (Table 3). There was a significant difference for Microstate 1 across age groups ( $F(2) = 6.00$ ,  $p = .01$ ,  $\eta^2 = .30$ ). Tukey's HSD post hoc tests (Table 4) revealed that coverage for Microstate 1 differed significantly between 8-months and 10-months, with Microstate 1 having a 20.50% coverage at 8-months and a 11.32% coverage at 10-months (Table 5). There was no significant difference for Microstate 2 across age groups ( $F(2) = 0.33$ ,  $p = .72$ ,  $\eta^2 = .02$ ), indicating that the percentage of coverage in Microstate 2 remained relatively stable across age groups. There was a significant difference for Microstate 3 across age groups ( $F(2) = 3.39$ ,  $p = .05$ ,  $\eta^2 = .18$ ). Tukey's HSD post hoc test revealed that coverage for Microstate 3 differed significantly between 8-months and 10-months, with Microstate 3 having a 21.78% coverage at 8-months and a 36.13% coverage at 10-months (Table 5). Lastly, there was no significant difference for Microstate 4 across age groups ( $F(2) = 2.37$ ,  $p = .11$ ,  $\eta^2 = .13$ ), indicating that the percentage of coverage in Microstate 4 remained fairly stable across age groups.

### 3.6. Transition probabilities

Transition probabilities were examined to ascertain the likelihood of transitioning from one microstate to another. A model of transitions among microstates for each of the three age groups are depicted in Fig. 4.A. Additionally, transition probabilities that showed a statistically significant difference across the three age groups with direction of change are shown in Fig. 4.B. There were statistically significant differences in transition probabilities between 6- and 8-months of age, with 8-months having significantly higher transition probabilities: from Microstate 2-1 ( $p = .01$ , 95% C.I. =  $[-0.08, -0.01]$ ), Microstate 3-1 ( $p = .02$ , 95% C.I. =  $[-0.09, -0.01]$ ), and Microstate 4-1 ( $p = .04$ , 95% C.I. =  $[-0.09, -0.003]$ ). There were also statistically significant differences in transition probabilities between 8- and 10-months of age. Transition probabilities moving from Microstate 2-1 ( $p = .001$ , 95% C.I. =  $[-0.12, -0.03]$ ) as well as moving from Microstate 4-1 ( $p = .02$ , 95% C.I. =  $[-0.11, -0.01]$ ) were significantly higher at 8 months than at 10 months. However, transition probabilities were significantly higher at 10-months than at 8-months when transitioning from Microstate 2-3 ( $p = .004$ , 95% C.I. =  $[0.03, 0.17]$ ) and Microstate 4-3 ( $p = .04$ , 95% C.I. =  $[0.003, 0.18]$ ). There were no significant differences between transition probabilities between 6- and 10-months.

### 3.7. Exploratory analyses: associations with temperament

Simple correlations were computed to explore relations between microstate parameters and IBQ-R scores (Tables 6–8). At the broadband level, Surgency/Positive Affectivity (Table 6) was negatively correlated with frequency ( $r(23) = -0.48$ ,  $p = .02$ ) and duration ( $r(23) = -0.43$ ,  $p = .03$ ) of microstate 3, indicating that infants with parent-ratings of higher surgency/positive affect were less likely to move into microstate 3 and, when microstate 3 did appear, they were less likely to stay in that topographic state. Looking at the narrowband scales, Smiling and Laughter was negatively correlated with frequency ( $r(23) = -0.48$ ,  $p = .02$ ) of microstate 3 and positively correlated with duration ( $r(23) = 0.50$ ,  $p = .01$ ) of microstate 1. High-Intensity Pleasure was also negatively correlated with frequency of microstate 3 ( $r(23) = -0.47$ ,  $p = .02$ ). Approach was negatively correlated with frequency ( $r(23) = -0.47$ ,  $p = .02$ ) and coverage ( $r(23) = -0.43$ ,  $p = .03$ ) of microstate 3, while it was positively correlated with duration ( $r(23) = 0.43$ ,  $p = .03$ ) and coverage ( $r(23) = 0.45$ ,  $p = .02$ ) of microstate 2.

Regarding the Negative Emotionality broadband score (Table 7), it was negatively correlated with coverage ( $r(23) = -0.51$ ,  $p = .01$ ) and duration ( $r(23) = -0.49$ ,  $p = .01$ ) of microstate 4 but positively correlated with GFP ( $r(23) = 0.43$ ,  $p = .03$ ) of microstate 3. At the narrowband level, Distress to Limitations was positively correlated with GFP ( $r(23) = 0.42$ ,  $p = .04$ ) of microstate 3 and negatively correlated with duration ( $r(23) = -0.46$ ,  $p = .02$ ) of microstate 4. Sadness was positively correlated with GFP ( $r(23) = 0.42$ ,  $p = .04$ ) of microstate 3 but negatively correlated with duration ( $r(23) = -0.40$ ,  $p = .045$ ) and coverage ( $r(23) = -0.49$ ,  $p = .01$ ) of microstate 4.

Lastly, Regulatory Capacity/Orienting (Table 8) was negatively correlated with coverage ( $r(23) = -0.40$ ,  $p = .049$ ) and frequency ( $r(23) = -0.44$ ,  $p = .03$ ) of microstate 2. With respect to component narrowband scales, Soothability was negatively correlated with frequency ( $r(23) = -0.57$ ,  $p = .003$ ), duration ( $r(23) = -0.44$ ,  $p = .03$ ), and coverage ( $r(23) = -0.58$ ,  $p = .002$ ) of microstate 2, while positively correlated with duration ( $r(23) = 0.51$ ,  $p = .01$ ) of microstate 3. Cuddliness was positively correlated ( $r(23) = 0.44$ ,  $p = .03$ ) with microstate 4.

In summary, a number of associations with temperament scores were observed, indicating that affective/motivational and

**Table 3**  
One-way ANOVA for Coverage with regard to Age and Microstate Topography.

	df	F	p value
Microstate 1	2	6.00	0.01 *
Microstate 2	2	0.33	0.72
Microstate 3	2	3.39	0.05 *
Microstate 4	2	2.37	0.11

**Table 4**  
Post Hoc Tests for Coverage.

	8-months	10-months
Microstate 1		
6-months	0.24	0.12
8-months		0.005 <sup>a</sup>
Microstate 2		
6-months	0.94	0.70
8-months		0.83
Microstate 3		
6-months	1.00	0.06
8-months		0.05 <sup>a</sup>
Microstate 4		
6-months	0.35	0.10
8-months		0.54

Note. These are the p-values for each comparison at each age.

<sup>a</sup> denotes significance.

**Table 5**  
Percentages of Coverage Time across Age and Microstate Topography.

	Microstate 1	Microstate 2	Microstate 3	Microstate 4
6-months	16.98%	31.66%	21.66%	29.70%
8-months	20.50%	30.35%	21.78%	27.37%
10-months	11.32%	27.41%	36.13%	25.15%

attention/regulation attributes were related to microstate parameters, as anticipated. There was a medium average effect size for the significant correlations ( $r^2 = 0.21$ ) ranging from small ( $r^2 = 0.06$ ) to large ( $r^2 = 0.34$ ). The largest effect sizes emerged for the significant positive correlation between Soothability and duration of microstate 3 ( $r^2 = 0.26$ ) as well as the negative correlations between Soothability and frequency of microstate 2 ( $r^2 = 0.32$ ) and coverage of microstate 2 ( $r^2 = 0.34$ ). All three factors were found to have medium to large effect sizes for different microstate topographies and their parameters. For the Positive Affect factor, there was a medium effect size for the correlation between the broadband score and frequency of microstate 3 ( $r^2 = 0.23$ ). The correlations between Negative Emotionality and coverage of microstate 4 had a large effect size ( $r^2 = 0.26$ ), with a medium effect size for duration of microstate 4 ( $r^2 = 0.24$ ). For Regulatory Capacity/Orienting, correlations between the factor score and frequency of microstate 2 ( $r^2 = 0.19$ ) as well as coverage of microstate 2 ( $r^2 = 0.16$ ) were consistent with a medium effect size.

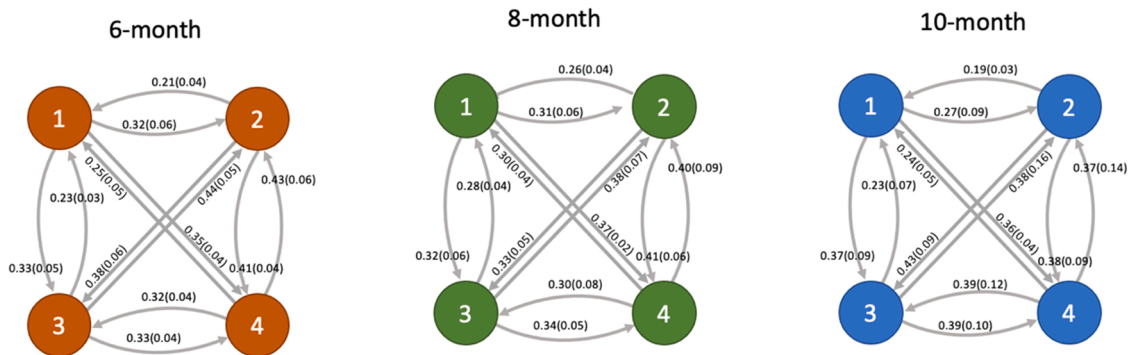
#### 4. Discussion

The present study aimed to identify microstates in infancy and to examine changes in microstate parameters over the second half of the first year of life. Microstates 2, 3, and 4 have topographies that closely replicate microstate topographies found in previous work in childhood and adulthood (Koenig et al., 2002). These microstates showed activation across the entirety of the scalp with differing orientations. Microstate 2 showed a symmetric occipital to prefrontal orientation and has been linked with attention engagement (Gui et al., 2021). Specifically, it has been suggested that Microstate 2 reflects a portion of the default mode network, which becomes activated in the absence of a task and decreases during performance of a cognitive task (Michel & Koenig, 2018). Microstate 3 had a left occipital to right frontal orientation, which has been suggested to be involved in auditory processing (Seitzman et al., 2017). Microstate 4, with its right occipital to left frontal orientation, has been observed in relation to visual stimuli and is associated with the activation of the visual system (Seitzman et al., 2017). Microstate 1 had a topography that had isolated activation at the posterior region. Given the isolated neural activity, it could be that this topography is unique in infancy and suggests localized, heightened activity in the parietal lobe that is much greater than other activity occurring across the scalp. Notably, this microstate topography was found in a previous study examining microstates in infancy with a social task (Gui et al., 2021). It could also be that this microstate is a result of artifact that was not removed from the data and does not correspond with underlying neural activity.

The resting state task in the current study involved watching a short clip of "Baby Einstein" which consisted of a video clip that the infants watched and listened to and is considered to invoke a calm state. The microstates found in this study appear to correspond with the cognitive processes needed to attend to the baseline task, involving auditory and visual processing while also invoking an attentive, yet calm state that does not require significant cognitive processes. Microstate 2, in particular, has been suggested to represent activation of the default mode network. The presence of this microstate during the baseline task could indicate that infants are reacting to this task as a resting or baseline condition in terms of their cortical network activity, consistent with expectations regarding its use.

There has been considerable exploration of the resting state tasks that are typically utilized in neuroimaging studies (e.g., Anderson & Perone, 2018; Camacho et al., 2020). When studying the developmental trajectory of the resting baseline task, one must consider how the brain reacts to "rest" as humans develop. One major line of questioning surrounds comparisons across the lifespan and considering if the resting task is indeed measuring a resting state that is comparable across different age groups. Camacho et al. (2020)

### A. Transition probabilities at each age group.



### B. Significant Differences in Connections

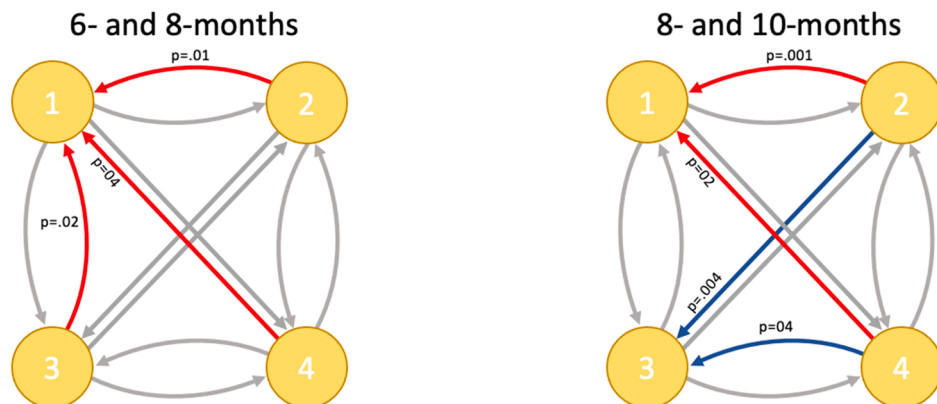


**Fig. 4.** A. Transition probabilities at each age group. Fig. 4 B. Significant Differences in Connections.

**Note.** Fig. 4A) The numbers outside of the parentheses represent the means and the numbers within the parentheses are the standard deviations.

Fig. 4.B) The presented values are p-values. The red arrow indicates that 8-months was significantly higher, while the blue arrow indicates that 10-months was significantly higher.

argue that baseline tasks during early development require a specific amount of control – to capture attention and create an engaging, yet cognitively routine, activity that limits additional cognitions (e.g., movement and distractions) from interfering. Given the microstate topographies, especially Microstate 2 emerging during this task, it seems that infants can maintain attention, yet fall into a cognitively similar resting state that is similar across the lifespan and corresponds with the default mode network (Panda et al., 2016).

When considering the microstate parameters, some interesting patterns emerged, particularly with Microstate 3. At 6 and 8 months, Microstate 3's duration remained relatively low compared to other microstates and stable. However, there was a significant increase in Microstate 3's duration at 10 months of age. This indicates that Microstate 3, once becoming activated remains active, on average, for a longer period of time, which is thought to correspond with the underlying network's stability. Microstate 3 was found to have significantly more coverage in 10-month-old infants compared to at 6- and 8-months. In fact, we found that more than 1/3rd (36.13%) of the task was spent in Microstate 3 compared to just over 1/5th at 6- (21.66%), and 8-months (21.78%). Notably, frequency for microstate 3 compared to microstate 4 was significantly lower. There appears to be an increase in the frequency of microstate 3 at 10-months closing the gap between microstates 3 and 4 (Fig. 3). However, this did not emerge as a significant interaction. Given that Microstate 3 is associated with auditory and phonological processing, the current microstate analysis indicates that these functions become particularly salient at about 10 months old, around the time infants begin to discern language and also appear more neurally

**Table 6**

Correlations between IBQ-R Surgency/Positive Affectivity with Narrowband domains and Microstate Parameters.

		SPA	ACT	SL	HP	VR	PS	APP
GFP1	<i>Pearson's r</i>	0.281	0.150	0.296	0.314	0.112	0.138	0.113
	<i>p-value</i>	.173	0.475	0.150	0.127	0.593	0.510	0.590
GFP2	<i>Pearson's r</i>	0.343	0.285	0.235	0.207	0.269	0.085	0.256
	<i>p-value</i>	.093	0.167	0.258	0.320	0.194	0.686	0.217
GFP3	<i>Pearson's r</i>	0.161	0.081	0.035	0.371	-0.103	0.056	0.228
	<i>p-value</i>	.442	0.700	0.869	0.068	0.623	0.791	0.272
GFP4	<i>Pearson's r</i>	0.334	0.189	0.119	0.336	0.287	0.102	0.244
	<i>p-value</i>	.103	0.367	0.341	0.101	0.164	0.627	0.239
Freq1	<i>Pearson's r</i>	0.022	-0.179	0.209	0.060	-0.048	0.157	-0.119
	<i>p-value</i>	.917	0.392	0.317	0.777	0.822	0.454	0.569
Freq2	<i>Pearson's r</i>	0.214	0.215	-0.091	0.175	0.075	0.077	0.350
	<i>p-value</i>	.305	0.301	0.664	0.402	0.721	0.713	0.086
Freq3	<i>Pearson's r</i>	-0.477	-0.220	-0.480	-0.465	-0.061	-0.150	-0.474
	<i>p-value</i>	.016a	0.291	0.015a	0.019a	0.773	0.475	0.017a
Freq4	<i>Pearson's r</i>	-0.046	-0.057	-0.171	0.017	0.046	0.010	0.001
	<i>p-value</i>	.827	0.788	0.414	0.934	0.827	0.961	0.996
Dur1	<i>Pearson's r</i>	0.353	0.063	0.502	0.306	0.150	0.215	0.141
	<i>p-value</i>	.084	0.763	0.010 * *	0.137	0.475	0.301	0.502
Dur2	<i>Pearson's r</i>	0.314	0.292	0.118	0.166	-0.053	0.156	0.431
	<i>p-value</i>	.126	0.156	0.575	0.427	0.802	0.457	0.031a
Dur3	<i>Pearson's r</i>	-0.353	-0.219	-0.154	-0.210	-0.145	-0.247	-0.332
	<i>p-value</i>	.083	0.293	0.463	0.313	0.489	0.234	0.105
Dur4	<i>Pearson's r</i>	-0.004	0.063	0.311	0.053	-0.086	-0.195	-0.107
	<i>p-value</i>	.987	0.765	0.130	0.800	0.681	0.351	0.661
Cov1	<i>Pearson's r</i>	0.181	-0.072	0.372	0.205	0.035	0.168	0.007
	<i>p-value</i>	.387	0.733	0.067	0.325	0.869	0.423	0.972
Cov2	<i>Pearson's r</i>	0.298	0.285	-0.001	0.188	0.044	0.121	0.450
	<i>p-value</i>	.148	0.167	0.995	0.368	0.833	0.565	0.024a
Cov3	<i>Pearson's r</i>	-0.425	-0.227	-0.329	-0.380	-0.063	-0.192	-0.429
	<i>p-value</i>	.034a	0.275	0.108	0.061	0.765	0.359	0.032a
Cov4	<i>Pearson's r</i>	-0.057	-0.017	0.046	0.032	-0.021	-0.128	-0.077
	<i>p-value</i>	.785	0.936	0.828	0.881	0.921	0.541	0.713

Note. The labels in the left column correspond to the 4 parameters and 4 microstates. SPA = Surgency/Positive Affectivity; ACT = Activity; SL = Smiling and Laughter; HP = High-Intensity Pleasure; VR = Vocal Reactivity; PS = Perceptual Sensitivity; APP = Approach.

<sup>a</sup> denotes significance.

activated by an auditory activity. As infants approach 10-months of age, there is considerable development in the auditory domain due to more complex language skills “coming online”. Generally, these findings suggest that the 10-month infant brain is generally becoming more activated by the music in the task than what was seen at 6- and 8-months.

Given that the Baby Einstein baseline task consists of a video with music playing, one might wonder how language processing corresponds with processing music. There has been research that links differences in musical notes, pitch, and meter to phonological and speech processing (Zhao & Kuhl, 2016). In a recent literature review by Morgan and Wren (2018), authors identified an increase in phonological acquisition and linguistic complexity that occurs from 9 months to 18 months of age. Taken together, the previous literature seems to align with the findings in this study that there is an increase in auditory processing, specifically with more complex processing that comes online between 8- and 10-months and leads to changes in the underlying auditory networks when confronted with a task that pulls for auditory processing.

When considering transition probabilities, it became clear that Microstate 1 and its potentially artifact laden topography impacted transition probabilities, especially in the 8-month population. All statistically significant transition probabilities that emerged as higher for 8-months than 6- and 10-months appeared when moving into Microstate 1. Additionally, the findings for frequency also revealed that microstate 1 was appearing in the data significantly less frequently as microstates 2, 3, and 4. This, in addition to the findings for coverage with microstate 1 having significantly more coverage in 8-months than 10-months, provides yet another piece of evidence that Microstate 1 appeared most often in the 8-month group. This pattern of results could mean that the remaining artifact that impacted this topography was most pervasive in this age group. However, it may also be that the microstate unique to our baseline condition (relative to other microstate investigations) or infant brain development is particularly salient during this time. Of note, the study of 8-month-old infants during a social go/no-go task by Gui et al. found a similar microstate to the present study’s microstate 1 (2021). There were other potentially interesting transition probabilities emerging between 8- and 10-months. Specifically, transitions into Microstate 3 appeared to happen more often at 10-months compared to 8-months of age. Given the significant increases in other microstate parameters for Microstate 3, this finding does not come as a surprise. With Microstate 3 corresponding with auditory/language processing, it seems that the probability of transitioning into this network is significantly higher at 10-months than at 8-months. Additionally, it seems that Microstate 3 is activated more often (higher frequency) and for longer periods of time (higher duration), perhaps indicating that between 8- and 10-months of age, this underlying network is strengthened, and the brain is much more attuned to pick up on the auditory aspects of the baseline task.

**Table 7**

Correlations between IBQ-R Negative Emotionality with Narrowband domains and Microstate Parameters.

		NA	DL	Fear	Fall	Sad
GFP1	<i>Pearson's r</i>	0.215	0.201	0.016	-0.152	0.292
	<i>p-value</i>	.302	0.335	0.939	0.468	0.157
GFP2	<i>Pearson's r</i>	0.230	0.242	0.026	-0.180	0.270
	<i>p-value</i>	.269	0.245	0.902	0.390	0.192
GFP3	<i>Pearson's r</i>	0.426	0.242	0.229	-0.271	0.419
	<i>p-value</i>	.034a	0.035a	0.270	0.190	0.037a
GFP4	<i>Pearson's r</i>	0.161	0.227	0.031	-0.098	0.151
	<i>p-value</i>	.441	0.274	0.883	0.641	0.471
Freq1	<i>Pearson's r</i>	0.317	0.285	0.104	-0.381	0.266
	<i>p-value</i>	.123	0.168	0.620	0.060	0.198
Freq2	<i>Pearson's r</i>	0.139	0.216	-0.073	-0.133	0.158
	<i>p-value</i>	.508	0.300	0.727	0.527	0.449
Freq3	<i>Pearson's r</i>	-0.200	-0.271	0.071	0.258	-0.188
	<i>p-value</i>	.338	0.190	0.737	0.212	0.368
Freq4	<i>Pearson's r</i>	-0.282	-0.152	-0.174	0.254	-0.315
	<i>p-value</i>	.172	0.467	0.404	0.221	0.125
Dur1	<i>Pearson's r</i>	0.205	0.164	0.076	-0.194	0.220
	<i>p-value</i>	.325	0.433	0.718	0.352	0.291
Dur2	<i>Pearson's r</i>	0.080	0.070	0.077	-0.038	0.067
	<i>p-value</i>	.705	0.740	0.715	0.857	0.750
Dur3	<i>Pearson's r</i>	-0.061	-0.139	0.172	0.165	-0.070
	<i>p-value</i>	.772	0.507	0.411	0.429	0.739
Dur4	<i>Pearson's r</i>	-0.488	-0.456	-0.354	0.352	-0.404
	<i>p-value</i>	.013	0.022a	0.083	0.084	0.045a
Cov1	<i>Pearson's r</i>	0.347	0.306	0.094	-0.388	0.332
	<i>p-value</i>	.089	0.136	0.655	0.055	0.105
Cov2	<i>Pearson's r</i>	0.137	0.182	-0.012	-0.117	0.143
	<i>p-value</i>	.515	0.384	0.953	0.577	0.494
Cov3	<i>Pearson's r</i>	-0.146	-0.221	0.124	0.222	-0.152
	<i>p-value</i>	.487	0.289	0.554	0.285	0.468
Cov4	<i>Pearson's r</i>	-0.507	-0.395	-0.342	0.394	-0.486
	<i>p-value</i>	.010	0.050	0.094	0.052	0.014a

Note. The labels in the left column correspond to the 4 parameters and 4 microstates. NA = Negative Emotionality; DL = Distress to Limitations; Fear = Fear; Fall = Falling reactivity; Sad = Sadness.

<sup>a</sup> denotes significance.

Exploratory analyses examining links between microstate parameters and temperament revealed a number of potentially important connections between emotional reactivity as well as attention-based regulation and underlying whole brain functionality. Microstate 3 was negatively correlated with the Surgency/Positive Affectivity broadband scale on the IBQ-R, while positively correlated with the Negative Emotionality. Specifically, the strength of the activation of microstate 3 was associated with higher parent ratings of overall Negative Emotionality, as well as fine-grained attributes of Distress to Limitations and Sadness. At a more fine-grained examination of Surgency/Positive Affectivity, higher frequency of microstate 3 was associated with lower Smiling and Laughter, High-Intensity Pleasure, and Approach tendencies. Additionally, higher coverage of microstate 3 was associated with lower Approach while higher duration and coverage of microstate 2 were associated with higher Approach ratings. Longer duration of microstate 1 was associated with greater Smiling and Laughter - an interesting pattern given the isolated topography of microstate 1 in the posterior region of the head, thought to correspond with activation in the visual cortex. This often-neglected microstate emerged in Gui et al.'s research examining social engagement in infants with and without autism, thus could be meaningful despite validity questions and awaits additional research for a more conclusive interpretation. For Regulatory Capacity/Orienting broadband, there was a negative correlation with coverage and frequency of microstate 2. At the narrowband level, higher levels of Soothability were associated with lower frequency, duration, and coverage of microstate 2 but longer duration of microstate 3. Increased Cuddliness was associated with longer durations of microstate 4. Associations between these microstates and temperament attributes is especially interesting given that cognitive functions have been previously associated with underlying networks linked with similar microstates. For example, microstate 3 topography has been associated with BOLD negative activations in the areas involved in phonological processing (Britz et al., 2010). Microstate 2 topography has been linked to positive BOLD activations in areas implicated in the salience network, which plays a critical role in switching between central executive function and the default mode (Britz et al., 2010; Sridharan et al., 2008). Overall, correlations in this study were associated with medium to large effect sizes pointing to differentiated relationships between microstate topographies/parameters and early temperament domains and indicating that microstates could be leveraged as biomarkers of temperament. Although temperament is generally thought of as affective/motivational in nature, attention-based regulation is included alongside reactivity in the psychobiological model, with infant temperament predicting later cognitive abilities, including executive functions, school-readiness, and language (Dixon & Smith, 2000; Gartstein et al., 2016; Rothbart et al., 2006). Thus, associations observed herein can be interpreted as supporting the importance of microstates for understanding the neuropsychological underpinnings of emotion-cognition connections.

**Table 8**

Correlations between IBQ-R Regulatory Capacity/Orienting with Narrowband domains and Microstate Parameters.

		RCO	DO	LP	Sooth	Cud
GFP1	<i>Pearson's r</i>	0.223	0.137	0.241	0.045	0.178
	<i>p-value</i>	.284	0.513	0.246	0.829	0.395
GFP2	<i>Pearson's r</i>	-0.104	-0.027	0.029	-0.345	0.055
	<i>p-value</i>	.622	0.898	0.889	0.091	0.793
GFP3	<i>Pearson's r</i>	-0.109	-0.002	-0.026	-0.215	-0.095
	<i>p-value</i>	.605	0.993	0.903	0.302	0.650
GFP4	<i>Pearson's r</i>	-0.047	0.017	0.098	-0.270	-0.008
	<i>p-value</i>	.825	0.937	0.643	0.192	0.969
Freq1	<i>Pearson's r</i>	0.316	0.338	0.083	0.253	0.162
	<i>p-value</i>	.124	0.098	0.695	0.222	0.439
Freq2	<i>Pearson's r</i>	-0.439	-0.346	-0.068	-0.565	-0.237
	<i>p-value</i>	.028a	0.909	0.746	0.003a	0.254
Freq3	<i>Pearson's r</i>	0.052	0.024	-0.023	0.259	-0.146
	<i>p-value</i>	.806	0.909	0.914	0.212	0.487
Freq4	<i>Pearson's r</i>	-0.160	-0.187	0.051	-0.218	-0.085
	<i>p-value</i>	.443	0.371	0.808	0.294	0.688
Dur1	<i>Pearson's r</i>	0.340	0.351	0.040	0.254	0.299
	<i>p-value</i>	.096	0.085	0.848	0.220	0.146
Dur2	<i>Pearson's r</i>	-0.209	-0.090	-0.031	-0.436	-0.025
	<i>p-value</i>	.316	0.669	0.882	0.029a	0.904
Dur3	<i>Pearson's r</i>	0.130	0.074	-0.178	0.508	-0.017
	<i>p-value</i>	.535	0.726	0.395	0.010a	0.935
Dur4	<i>Pearson's r</i>	0.196	-0.075	0.128	0.191	0.436
	<i>p-value</i>	.348	0.721	0.541	0.361	0.030a
Cov1	<i>Pearson's r</i>	0.377	0.375	0.127	0.283	0.225
	<i>p-value</i>	.063	0.065	0.544	0.171	0.279
Cov2	<i>Pearson's r</i>	-0.398	-0.266	-0.072	-0.581	-0.190
	<i>p-value</i>	.049a	0.199	0.734	0.002a	0.363
Cov3	<i>Pearson's r</i>	0.103	0.073	-0.095	0.390	-0.095
	<i>p-value</i>	.625	0.730	0.653	0.054	0.651
Cov4	<i>Pearson's r</i>	-0.001	-0.190	0.117	-0.037	0.194
	<i>p-value</i>	.996	0.362	0.578	0.861	0.352

Note. The labels in the left column correspond to the 4 parameters and 4 microstates. RCO = Regulatory Capacity/Orienting; DO = Duration of Orienting; LP = Low-Intensity Pleasure; Sooth = Soothability; Cud = Cuddliness.

<sup>a</sup> denotes significance.

The emergence of microstates in infancy demonstrated in this study indicates the need for additional research exploring the manner in which microstates interact with key domains of cognitive, emotional and motor functioning, which lends itself to a dynamic systems theory lens. Dynamic systems theory generally relates to one's ability to integrate aspects of functioning to behave appropriately in a given context, and recently, this framework was used to explain the development of executive functioning (Perone et al., 2021). Starting in early childhood, we begin to see the emergence of goal-directed behavior and how this behavior builds into more complex functioning over time. These intentional behaviors integrate neural activity, motor activity, emotion regulating processes, etc., to achieve the desired outcome. Over time, we activate these systems more and more, continuing to strengthen the underlying patterns leading to a higher probability of moving into that system when situations arise. As this system "comes online", its continual use and strengthening is thought to create a "preferred state" (Perone et al., 2021), which could be linked with microstate topography and parameters such as coverage and frequency. These ideas emerging from dynamic systems theory provide an effective framework for an enhanced understanding of microstate emergence and development, or vice versa. Perhaps, microstates could provide insight into the neural correlates of these dynamic systems their identification in infancy can advance related research.

Overall, this study found that microstates can be extracted from infant EEG data. Using a baseline task comprised of a stimulating video with dynamic images and sound, three microstates emerged that appear comparable to the underlying networks identified in the adult microstate literature (Michel & Koenig, 2018) as well as infant fMRI studies (Gao et al., 2017; Fransson et al., 2007). This number of microstates also corresponds with what was found in previous infant microstates literature (Gui et al., 2021; Maitre et al., 2021). These networks were found in the previous literature to correspond with auditory and visual processing as well as the default mode network. Interestingly, Microstate 3, thought to correspond with auditory/language processing, increased across parameters at 10-months compared to 6- and 8-months of age. At 10 months of age, Microstate 3 was becoming activated more often, for longer periods of time, covering significantly more of the entirety of the task, and was more likely to be transitioned into. These findings seem to correspond with previous literature examining language acquisition and phonological processing that comes online around this age (Huttenlocher, 1974; Benedict, 1979; Gervain & Mehler, 2010; Morgan & Wren, 2018).

## 5. Limitations

This study, while having important findings, was not without limitations. As with all EEG work, there are limitations that come with

measuring brain activity in this way. Spatial resolution of brain activity is not as precise as temporal resolution and because EEG measures electrical activity on the scalp, it does not provide an optimal representation of more deeply located signal sources. Another limitation is that the sample size for this study was small. While this is not uncommon in previous literature examining microstates (Michel & Koenig, 2018), more current literature (e.g., Gui et al., 2021) has much larger sample sizes. Having a larger sample size would increase generalizability of the study and allow for more reliable findings with greater statistical power and eliminating the possibility of sample or equipment specific results. Because examining correlations between temperament and microstate topographies and parameters were largely exploratory, corrections for multiple statistical tests were not implemented in order to ensure adequate statistical power with a relatively small sample. Future studies with larger samples should make such adjustments or pursue more precise hypothesis testing based on the present findings. Additionally, this study utilizes a cross-sectional design which limits our ability to speak to developmental processes. Utilizing a longitudinal approach is necessary to elucidate the stability of microstates and to ascertain their connection to cognitive and emotional milestones across development. This study did not include behavioral correlates of the infants while attending to the baseline task. This limits the conclusion of this study to what has been found in previous literature, specifically adult microstate literature and fMRI studies. In future studies, a consideration of the specific behaviors during tasks should be considered to better understand the functional significance of the microstates.

## 6. Future directions

This study found discrete microstates that emerged in infancy, which can lead to new investigations examining differences across stimulus presentations to further explain how infants begin to recognize, respond to, and engage with the world around them. Given the microstates identified in this study and their relation to underlying networks, which appear to be engaged in responding to the baseline task (attention, resting state, visual, and auditory processing), additional coordinated activity could be elucidated by utilizing structured tasks eliciting specific cognitions and/or emotional experiences. Ultimately, these findings can add to the knowledge regarding the neurodevelopment of global networks and allows for comparisons across the lifespan. This work begins establishing microstates as a methodological approach for longitudinal studies of individual differences in brain development. Additionally, the exploratory analyses examining microstates and temperament offer a vast line of research that can now be explored more intentionally with hypotheses about emotional and temperamental reactions to certain tasks and stimuli. Microstates could be utilized to advance the study of the intersection between cognition and emotion, specifically examining microstate differences through the lens of whole brain networks related to positive and negative affect, and links with reactivity/regulation related attributes. Given the identification of the relationship between microstates and temperament during a resting-state task, more nuanced stimuli could be introduced to evoke emotional states and measure changes in underlying brain networks and microstate parameters.

This line of research acts as a foundation for microstates research across the lifespan and is necessary to understand their emergence and the origins of the underlying global neural networks. This addition to the literature can improve our understanding of findings obtained in childhood and adulthood. Given the relationship between resting networks found in fMRI and microstates, future studies could examine stimulus related neural activity in infancy which was impossible to do with infants using fMRI.

## CRediT authorship contribution statement

**Kara L. Brown:** Conceptualization, Methodology, Investigation, Statistical analyses, Data curation, Writing – original draft, Revisions. **Maria A. Gartstein:** Conceptualization, Methodology, Investigation, Data curation, Writing – reviewing & editing.

## Data Availability

The data that has been used is confidential.

## Acknowledgments

We would like to acknowledge and thank the research assistants who were a part of the project and assisted with data collection and processing. Additionally, we would like to acknowledge and thank the families who participated in this project. Their time and effort made this work possible.

## References

Anderson, A. J., & Perone, S. (2018). Developmental change in the resting state electroencephalogram: Insights into cognition and the brain. *Brain and Cognition*, 126, 40–52. <https://doi.org/10.1016/j.bandc.2018.08.001>

Benedict, H. (1979). Early lexical development: comprehension and production. *Journal of Child Language*, 6(2), 183–200. <https://doi.org/10.1017/s0305000900002245>

Biswal, B., Yetkin, F., Haughton, V., & Hyde, J. (1995). Functional connectivity in the motor cortex of resting human brain using echo-planar MRI. *Magnetic Resonance in Medicine*, 34(4), 537–541. <https://doi.org/10.1002/mrm.1910340409>

Britton, J., Frey, L., Hopp, J., Frey, L., Korb, P., Koubeissi, M., Lievens, W., Pestana-Knight, E., & St. Louis, E. (2016). In E. St. Louis, & L. Frey (Eds.), *Electroencephalography (EEG): An introductory text and atlas of normal and abnormal findings in adults, children, and infants*. American Epilepsy Society. (<https://www.ncbi.nlm.nih.gov/books/NBK390354/>).

Britz, J., Van De Ville, D., & Michel, C. M. (2010). BOLD correlates of EEG topography reveal rapid resting-state network dynamics. *NeuroImage*, 52(4), 1162–1170. <https://doi.org/10.1016/j.neuroimage.2010.02.052>

Brodbeck, V., Kuhn, A., von Wegner, F., Morzelewski, A., Tagliazucchi, E., Borisov, S., Michel, C., & Laufs, H. (2012). EEG microstates of wakefulness and NREM sleep, 2012-09 *Neuroimage*, 62(3), 2129–2139. <https://doi.org/10.1016/j.neuroimage.2012.05.060>. Epub 2012 May 30.

Camacho, M. C., Quiñones-Camacho, L. E., & Perlman, S. B. (2020). Does the child brain rest?: An examination and interpretation of resting cognition in developmental cognitive neuroscience. *NeuroImage (Orlando, Florida)*, 212, Article 116688. <https://doi.org/10.1016/j.neuroimage.2020.116688>

Campagna, A. X., Pham, C., & Gartstein, M. A. (2021). Understanding emerging regulation: The role of frontal electroencephalography (EEG) asymmetry and negative affectivity. *Developmental Psychobiology*, 63, Article e22198. <https://doi.org/10.1002/dev.22198>

Cherian, J., Swarte, R., & Visser, G. (2009). Technical standards for recording and interpretation of neonatal electroencephalogram in clinical practice. *Annals of the Indian Academy of Neurology*, 12(1), 58–70. <https://doi.org/10.4103/0972-2327.48869>

Croce, P., Quercia, A., Costa, S., & Zappasodi, F. (2020). EEG microstates associated with intra- and inter-subject alpha variability. *Scientific Reports*, 10(1), 2469. <https://doi.org/10.1038/s41598-020-58787-w>

Cuevas, K., & Bell, M. A. (2014). Infant attention and early childhood executive function. *Child Development*, 85(2), 397–404. <https://doi.org/10.1111/cdev.12126>

Da Cruz, J. R., Favrod, O., Rojishvili, M., Chkonia, E., Brand, A., Mohr, C., et al. (2020). EEG microstates are a candidate endophenotype for schizophrenia. *Nature Communications*, 11(1), 3089. –3089.

Delorme, A., & Makeig, S. (2004). EEGLAB: an open source toolbox for analysis of single-trial EEG dynamics including independent component analysis. *Journal of Neuroscience Methods*, 134, 9–21. <https://doi.org/10.1016/j.jneumeth.2003.10.009>

Dixon, Wallace E. Jr., & Smith, P. Hul (2000). Links Between Early Temperament and Language Acquisition. *Merrill-Palmer Quarterly*.

Fox, M., & Raichle, M. (2007). Spontaneous fluctuations in brain activity observed with functional magnetic resonance imaging. *Nature Reviews Neuroscience*, 8, 700–711. <https://doi.org/10.1038/nrn2201>

Fransson, P., Sköld, B., Horsch, S., Nordell, A., Blennow, M., Lagercrantz, H., & Åden, U. (2007). Resting-state networks in the infant brain. *Proceedings of the National Academy of Sciences*, 104(39), 15531–15536. <https://doi.org/10.1073/pnas.0704380104>

Gao, W., Alcauter, S., Elton, A., Hernandez-Castillo, C., Smith, J., Ramirez, J., & Lin, W. (2015). Functional Network Development During the First Year: Relative Sequence and Socioeconomic Correlations. *Cerebral Cortex*, 25(9), 2919–2928. <https://doi.org/10.1093/cercor/bhu088>

Gao, W., Lin, W., Grewen, K., & Gilmore, J. H. (2017). Functional connectivity of the infant human brain: Plastic and modifiable. *The Neuroscientist: a Review Journal bringing Neurobiology, Neurology and Psychiatry*, 23(2), 169–184. <https://doi.org/10.1177/1073858416635986>

Gartstein, Masha A., Putnam, Samuel P., & Kliewer, Rachel (2016). Do Infant Temperament Characteristics Predict Core Academic Abilities in Preschool-Aged Children? *Learning and Individual Differences*, 45, 299–306. <https://doi.org/10.1016/j.lindif.2015.12.022>

Gartstein, & Rothbart, M. K. (2003). Studying infant temperament via the revised infant behavior questionnaire. *Infant Behavior & Development*, 26(1), 64–86. [https://doi.org/10.1016/S0163-6383\(02\)00169-8](https://doi.org/10.1016/S0163-6383(02)00169-8)

Gartstein, M. A. (2019). Frontal electroencephalogram (EEG) asymmetry: Exploring contributors to the Still Face procedure response. *International Journal of Behavioral Development*, 44, 193–204.

Gervain, J., & Mehler, J. (2010). Speech perception and language acquisition in the first year of life. *Annual Review of Psychology*, 61(1), 191–218. <https://doi.org/10.1146/annurev.psych.093008.100408>

Gianotti, L. R., Faber, P. L., Schuler, M., Pascual-Marqui, R. D., Kochi, K., & Lehmann, D. (2008). First valence, then arousal: The temporal dynamics of brain electric activity evoked by emotional stimuli. *Brain Topography*, 20(3), 143–156. <https://doi.org/10.1007/s10548-007-0041-2>

Greicius, M., Krasnow, B., Reiss, A., & Menon, V. (2002). Functional connectivity in the resting brain: A network analysis of the default mode hypothesis. *Proceedings of the National Academy of Sciences – PNAS*, 100(1), 253–258. <https://doi.org/10.1073/pnas.0135058100>

Gui, A., Bussu, G., Tye, C., Elsabagh, M., Pasco, G., Charman, T., Johnson, M. H., & Jones, E. J. H. (2021). Attentive brain states in infants with and without later autism. –196 *Translational Psychiatry*, 11(1), 196. <https://doi.org/10.1038/s41398-021-01315-9>.

Huttenlocher, J. (1974). The origins of language comprehension. In R. L. Solso (Ed.), *Theories in cognitive psychology: the Loyola Symposium* (pp. 331–368). Potomac, MD: Erlbaum.

Jia, H., & Yu, D. (2018). Aberrant intrinsic brain activity in patients with autism spectrum disorder: Insights from EEG microstates. *Brain Topography*, 32(2), 295–303. <https://doi.org/10.1007/s10548-018-0685-0>

Kaur, A., Chinnadurai, V., & Chaujar, R. (2020). Microstates-based resting frontal alpha asymmetry approach for understanding affect and approach/withdrawal behavior. *Scientific Reports*, 10(1), 4228. <https://doi.org/10.1038/s41598-020-61119-7>

Khanna, A., Pascual-Leone, A., & Farzan, F. (2014). Reliability of resting-state microstate features in electroencephalography. *PloS One*, 9(12), Article e114163. <https://doi.org/10.1371/journal.pone.0114163>

Khanna, A., Pascual-Leone, A., Michel, C. M., & Farzan, F. (2015). Microstates in resting-state EEG: Current status and future directions. *Neuroscience and Biobehavioral Reviews*, 49, 105–113. <https://doi.org/10.1016/j.neubiorev.2014.12.010>

Khazaei, M., Raeisi, K., Croce, P., Tamburro, G., Tokarev, A., Vanhatalo, S., Zappasodi, F., & Comani, S. (2021). Characterization of the functional dynamics in the neonatal brain during REM and NREM sleep states by means of microstate analysis. *Brain topography*, 34(5), 555–567. <https://doi.org/10.1007/s10548-021-00861-1>

Kikuchi, M., Koenig, T., Munessu, T., Hanaoka, A., Strik, W., Dierks, T., Koshino, Y., & Minabe, Y. (2011). EEG microstate analysis in drug-naïve patients with panic disorder. *PloS One*, 6(7), Article e22912. <https://doi.org/10.1371/journal.pone.0022912>

Koenig, T., Prichep, L., Lehmann, D., Sosa, P. V., Braecker, E., Kleindlogel, H., Isenhardt, R., & John, E. R. (2002). Millisecond by millisecond, year by year: Normative EEG microstates and developmental stages. *NeuroImage*, 16(1), 41–48. <https://doi.org/10.1006/nimg.2002.1070>

Lehmann, D., Faber, P. L., Galderisi, S., Herrmann, W. M., Kinoshita, T., Koukkou, M., Mucci, A., Pascual-Marqui, R. D., Saito, N., Wackermann, J., Winterer, G., & Koenig, T. (2005). EEG microstate duration and syntax in acute, medication-naïve, first-episode schizophrenia: A multi-center study. *Psychiatry Research Neuroimaging*, 138(2), 141–156. <https://doi.org/10.1016/j.pscychresns.2004.05.007>

Lehmann, D., Ozaki, H., & Pal, I. (1987). EEG alpha map series: brain micro-states by space-oriented adaptive segmentation. *Electroencephalography and Clinical Neurophysiology*, 67(3), 271–288. [https://doi.org/10.1016/0013-4694\(87\)90025-3](https://doi.org/10.1016/0013-4694(87)90025-3)

Lehmann, D., Strik, W. K., Henggeler, B., Koenig, T., & Koukkou, M. (1998). Brain electric microstates and momentary conscious mind states as building blocks of spontaneous thinking: I. Visual imagery and abstract thoughts. *International Journal of Psychophysiology*, 29(1), 1–11. [https://doi.org/10.1016/s0167-8760\(97\)00098-6](https://doi.org/10.1016/s0167-8760(97)00098-6)

Lopez-Calderon, J., & Luck, S. J. (2014). ERPLAB: An open-source toolbox for the analysis of event-related potentials. *Frontiers in Human Neuroscience*, 8, 213. <https://doi.org/10.3389/fnhum.2014.00213>

Maitre, N. L., Key, A. P., Slaughter, J. C., Yoder, P. J., Neel, M. L., Richard, C., Wallace, M. T., & Murray, M. M. (2020). Neonatal multisensory processing in preterm and term infants predicts sensory reactivity and internalizing tendencies in early childhood. *Brain topography*, 33(5), 586–599. <https://doi.org/10.1007/s10548-020-00791-4>

Meehan, T. P., & Bressler, S. L. (2012). Neurocognitive networks: Findings, models, and theory. *Neuroscience and Biobehavioral Reviews*, 36(10), 2232–2247. <https://doi.org/10.1016/j.neubiorev.2012.08.002>

Mele, G., Cavaliere, C., Alfano, V., Orsini, M., Salvatore, M., & Aiello, M. (2019). Simultaneous EEG-fMRI for functional neurological assessment. *Frontiers in Neurology*, 10, 848. <https://doi.org/10.3389/fneur.2019.00848>

Mesulam, M. (2012). The evolving landscape of human cortical connectivity: Facts and inferences. *NeuroImage*, 62(4), 2182–2189. <https://doi.org/10.1016/j.neuroimage.2011.12.033>

Michel, C. M., & Koenig, T. (2018). EEG microstates as a tool for studying the temporal dynamics of whole-brain neuronal networks: A review. *NeuroImage*, 180(Pt B), 577–593. <https://doi.org/10.1016/j.neuroimage.2017.11.062>

Milz, P., Faber, P., Lehmann, D., Koenig, T., Kochi, K., & Pascual-Marqui, R. (2016). The functional significance of EEG microstates—Associations with modalities of thinking. *NeuroImage*, 125, 643–656. <https://doi.org/10.1016/j.neuroimage.2015.08.023>

Morgan, L., & Wren, Y. E. (2018). A systematic review of the literature on early vocalizations and babbling patterns in young children. *Communication Disorders Quarterly*, 40(1), 3–14. <https://doi.org/10.1177/1525740118760215>

Murphy, Whitton, A. E., Deccy, S., Ironside, M. L., Rutherford, A., Beltz, M., Sacchet, M., & Pizzagalli, D. A. (2020). Abnormalities in electroencephalographic microstates are state and trait markers of major depressive disorder. *Neuropsychopharmacology*, 45(12), 2030–2037. <https://doi.org/10.1038/s41386-020-0749-1>

Panda, R., Bharath, R. D., Upadhyay, N., Mangalore, S., Chennu, S., & Rao, S. L. (2016). Temporal dynamics of the default mode network characterize meditation-induced alterations in consciousness. *Frontiers in Human Neuroscience*, 10, 372. <https://doi.org/10.3389/fnhum.2016.00372>

Pascual-Marqui, R. D., Michel, C. M., & Lehmann, D. (1995). Segmentation of brain electrical activity into microstates: Model estimation and validation. *IEEE Transactions on Biomedical Engineering*, 42(7), 658–665. <https://doi.org/10.1109/10.391164>

Perone, S., Simmering, V. R., & Buss, A. T. (2021). A dynamical reconceptualization of executive-function development. *Perspectives on Psychological Science*. <https://doi.org/10.1177/1745691620966792>

Poulsen, A.T., Pedroni, A., Langer, N., & Hansen, L.K., (2018). Microstate EEGlab toolbox: An introductory guide. bioRxiv.

Raichle, M. E., MacLeod, A. M., Snyder, A. Z., Powers, W. J., Gusnard, D. A., & Shulman, G. L. (2001). A default mode of brain function. *Proceedings of the National Academy of Sciences - PNAS*, 98(2), 676–682. <https://doi.org/10.1073/pnas.98.2.676>

Rosenblum, K. L., Dayton, C. J., & Muzik, M. (2019). Infant social and emotional development. In C. Zeanah (Ed.), *Handbook of infant mental health* (Fourth edition., pp. 95–119). The Guilford Press.

Rothbart, M. K., & Derryberry, D. (1981). Development of individual difference in temperament. In M. E. Lamb, & A. L. Brown (Eds.), *Advances in developmental psychology* (pp. 37–86). Hillsdale, NJ: Lawrence Erlbaum Associates.

Rothbart, M. K., Posner, M. I., & Kieras, J. (2006). Temperament, attention, and the development of self-regulation. In K. McCartney, & D. Phillips (Eds.), *Blackwell handbook of early childhood development* (pp. 338–357). Blackwell Publishing. (<https://doi.org/10.1002/9780470757703.ch17>).

Seitzman, B. A., Abell, M., Bartley, S. C., Erickson, M. A., Bolbcker, A. R., & Hetrick, W. P. (2017). Cognitive manipulation of brain electric microstates. *NeuroImage (Orlando, Florida)*, 146, 533–543. <https://doi.org/10.1016/j.neuroimage.2016.10.002>

Smith, E. E., Reznik, S. J., Stewart, J. L., & Allen, J. J. (2017). Assessing and conceptualizing frontal EEG asymmetry: An updated primer on recording, processing, analyzing, and interpreting frontal alpha asymmetry. *International Journal of Psychophysiology*, 111, 98–114. <https://doi.org/10.1016/j.ijpsycho.2016.11.005>

Sridharan, D., Levitin, D. J., & Menon, V. (2008). critical role for the right fronto-insular cortex in switching between central-executive and default-mode networks. *Proceedings of the National Academy of Sciences - PNAS*, 105(34), 12569–12574. <https://doi.org/10.1073/pnas.0800005105>

Strelets, V., Faber, P. L., Golikova, J., Novototsky-Vlasov, V., Koenig, T., Gianotti, L. R. R., Gruzelier, J. H., & Lehmann, D. (2003). Chronic schizophrenics with positive symptomatology have shortened EEG microstate durations. *Clinical Neurophysiology*, 114(11), 2043–2051. [https://doi.org/10.1016/s1388-2457\(03\)00211-6](https://doi.org/10.1016/s1388-2457(03)00211-6)

Strik, W., Dierks, K., Becker, T., & Lehmann, D. (1995). Larger topographical variance and decreased duration of brain electric microstates in depression. *Journal of Neural Transmission*, 99(1–3), 213–222. <https://doi.org/10.1007/BF01271480>

Whedon, M., Perry, N. B., & Bell, M. A. (2020). Relations between frontal EEG maturation and inhibitory control in preschool in the prediction of children's early academic skills. *Brain and cognition*, 146, Article 105636. <https://doi.org/10.1016/j.bandc.2020.105636>

Winkler, I., Debecker, S., Müller, K., and Tangermann, M. (2015) On the influence of high-pass filtering on ICA-based artifact reduction in EEG-ERP, 37th Annual International Conference of the IEEE Engineering in Medicine and Biology Society (EMBC), 2015, pp. 4101–4105, doi: 10.1109/EMBC.2015.7319296.

Zerna, J., Strobel, A., & Scheffel, C. (2021). EEG microstate analysis of emotion regulation reveals no sequential processing of valence and emotional arousal. *Scientific Reports*, 11(1), 21277. <https://doi.org/10.1038/s41598-021-00731-7>

Zhao, T. C., & Kuhl, P. K. (2016). Musical intervention enhances infants' neural processing of temporal structure in music and speech. *Proceedings of the National Academy of Sciences of the United States of America*, 113(19), 5212–5217. <https://doi.org/10.1073/pnas.1603984113>